Mechanism of skyrmion condensation and pairing for twisted bilayer graphene

Dian Jing, Alexander Conkey Tyner, and Pallab Goswami

Phys. Rev. B **105**, 184505 — Published 5 May 2022

DOI: 10.1103/PhysRevB.105.184505

Mechanism of skyrmion condensation and pairing for twisted bi-layer graphene

Dian Jing[1,2,3], Alexander Conkey Tyner[4], Pallab Goswami[1,4]
[1] *Department of Physics and Astronomy, Northwestern University, Evanston, IL 60208*
[2] *Department of Chemical and Biological Engineering, Northwestern University, Evanston, IL 60208*
[3] *Integrated Science Program, Northwestern University, Evanston, IL 60208 and*
[4] *Graduate Program in Applied Physics, Northwestern University, Evanston, IL 60208*
(Dated: January 7, 2022)

When quantum flavor Hall insulator phases of itinerant fermions are disordered by strong quantum fluctuations, the condensation of skyrmion textures of order parameter fields can lead to superconductivity. In this work, we address the mechanism of skyrmion condensation by considering the scattering between (2+1)-dimensional, Weyl fermions and hedgehog-type tunneling configurations of order parameters that violate the skyrmion-number conservation law. We show the quantized, flavor Hall conductivity (σ^f_{xy}) controls the degeneracy of topologically protected, fermion zero-modes, localized on hedgehogs. The overlap between zero-mode eigenfunctions or 't Hooft vertex is shown to control the nature of paired states. Employing this formalism for the $N = 2$ model of twisted bilayer graphene, we describe the competition among flavor Hall orders, charge $4e^-$ $4e^-$ superconductivity, and various charge $2e^-$ paired states in BCS and pair-density-wave channels. At charge neutrality, we show that the competition between flavor Hall insulators and charge $2e^-$ states can be captured by $SO(9)$ non-linear sigma models. If topological pairing mechanism can dominate over conventional pairing mechanism, our work predicts the flavor-symmetry-preserving, charge $4e^-$ superconductivity as a natural candidate for the paired state in the vicinity of charge neutral point.

I. INTRODUCTION

Skyrmions are smooth, topologically non-trivial, textures of three-component, unit vector field $\hat{\mathbf{\Omega}}(\mathbf{x})$ of $O(3)$ non-linear sigma model (NLSM) at two spatial dimensions.[1] Since $\hat{\mathbf{\Omega}}(\mathbf{x})$ is equivalent to a two-sphere (S^2), the skyrmion configurations are classified by the second homotopy group: $\pi_2(S^2) = \mathbb{Z}$. Inside the ordered phase of NLSM, the skyrmion requires a finite creation energy $E_{sk} = 4\pi\rho_s|W_{sk}|$, where ρ_s is the spin-stiffness of the NLSM, and W_{sk} is the integer-valued, winding number. If $\hat{\mathbf{\Omega}}(\mathbf{x})$ is coupled to (2+1)-dimensional Weyl fermions as a mass type order parameter, the skyrmions can support induced "fermion numbers", indicating the presence of fluctuating competing orders inside the skyrmion core.[2–18] When the NLSM is disordered by quantum fluctuations, the vanishing of excitation gap can allow the condensation of skyrmions. Hence, the quantum-disordered, anti-ferromagnet (AFM) and quantum spin Hall (QSH) states can support nucleation of spin-singlet, valence bond solids (VBS)[8] and s-wave superconductivity,[9,13–15] respectively.

The analysis of such competing orders is often guided by the construction of $SO(5)$ NLSMs that treat spin-triplet and spin-singlet orders on an equal footing. After integrating out the gapped fermion fields, one obtains a non-Abelian, Berry's phase for the five-component vector field[6–16], which is also known as the Wess-Zumino-Witten (WZW) term. The relationship between $SO(5)$ WZW model and the unconventional, continuous quantum phase transitions between two ordered states[19] is being actively studied by many groups.[20–22]

Owing to the discovery of superconductivity in twisted bilayer graphene (TBLG) in the vicinity of correlated insulating states, the analysis of competing particle-hole and particle-particle orders of Weyl fermions has become an important, physically relevant problem.[23–35] The interactions between fermion fields and bosonic collective modes, such as phonons and smooth order parameter fluctuations are being vigorously investigated, as potential candidates for pairing mechanism.[36–43] Recently, the skyrmion condensation has also been considered for addressing the competition between correlated insulators and adjacent superconducting states.[44–47] Based on the low energy theories of 4− and 8− flavors of Weyl fermions, different types of level-1[44] and level-2[45] $SO(5)$ WZW models have been proposed for the integer filling fractions $\nu = 2$, and 0, respectively. The topological pairing mechanism can provide critical, non-perturbative insights into the nature of competing orders and emergent symmetries, which are generally inaccessible through perturbation theories about topologically trivial configurations of collective modes. This motivates us to ask the following question.

How do the skyrmions condense and determine the nature of competing orders? Due to the vanishing of E_{sk}, all topologically distinct ground states, labeled by different W_{sk}'s can become energetically degenerate. Such infinite degeneracy of ground states is removed by hedgehog or monopole type tunneling configurations of order parameter in Euclidean space-time. They violate the skyrmion-number conservation law and lead to a superposition of different skyrmion configurations as the true ground state.[48–50] Therefore, the mechanism of condensation and the nature of superconducting states cannot be clearly understood, without considering interactions between Weyl fermions and hedgehogs.

Furthermore, for $4N$-flavors of Weyl fermions with $N > 1$, a spin-triplet order has many competing spin-singlet, mass orders, which anti-commute with each other. Naturally, there are multiple candidates for level-N $SO(5)$ WZW theories, and they cannot provide an unbiased description of competing spin-singlet orders. Such issues for the $N = 2$ case were identified in Refs. 16,17, while addressing the competition between AFM, VBS, and Kondo-singlets. Ref. 17 has showed the space-time dependent, Weyl operator in the presence of hedgehog configurations of AFM order parameter possesses topologically protected fermion zero-modes. Many similarities between this problem and (3+1)-dimensional quantum chromodynamics[51,52] were pointed out. The overlap between zero-modes was shown to cause an effective $2N$-fermion interaction or 't Hooft vertex (TV).[53] For $N = 1$, TV is a frequency-momentum dependent fermion billinear, describing VBS order. For $N \geq 2$, the quartic TV corresponds to a composite, spin-singlet order, which cannot be described by VBS or Kondo-singlet type fermion bilinears.

The primary goal of our current work is to address the nature of paired states arising from the condensation of skyrmion textures of quantum flavor Hall (QFH) insulators for $4N$-flavors of Weyl fermions, by explicitly considering the role of hedgehogs. For the clarity of presentation, we will only consider triplet orders for one of the $SU(2)$ sub-groups of $SU(4N)$. In response to the externally applied electric fields, uniformly ordered, QFH states exhibit quantized Hall conductivity $\sigma^f_{xy} = 2N$ for the spin or valley type flavor currents. For TBLG, we will mainly focus on $\nu = 0$.

Our manuscript is organized as follows. In Sec. II, we set up the effective theory of $(2 + 1)$-dimensional, free Weyl fermions and outline its $U(4N) = SU(4N) \times U(1)$ flavor symmetry. The skyrmion texture and induced fermion number of QFH triplet insulating orders, which breaks one $SU(2)$ sub-group of $SU(4N)$, are discussed in Sec. III. The fermion zero modes of dynamic Weyl operator with hedgehog tunneling configurations and the $U(1)$ global symmetry breaking, pairing bilinears from zero mode channel are described in Sec. IV, and Sec. V, respectively. The dynamic 't Hooft vertex describing the flavor symmetric charge $2Ne^-$ state is constructed in Sec. VI. The effects of flavor-symmetry-breaking (FSB) for commensurate filling fractions away from charge neutrality are considered in Sec. VII. We conclude by discussing physical significance of our results in Sec. VIII. For technically non-inclined readers, the important physical results and predictions of our work are summarized in Table I and Figs. 2-4.

II. FLAVOR SYMMETRY OF WEYL FERMIONS

The low energy theory of many two-dimensional systems can be described by multiple species of linearly dispersing Weyl fermions. The Weyl points with chirality $+1$ (-1) act as unit strength vortices (anti-vortices) in momentum space. In this work, we denote them as the right- and the left- handed Weyl points, respectively, which come in pairs, due to the fermion doubling theorem. On a general ground, we will consider $2N$ pairs of right- and left- handed fermions, where the factor of 2 (N) counts for the spin (layer or other internal) degrees of freedom. We will describe the two-component, right-handed and left-handed fermion fields by $R^T_{i,s}(t,\boldsymbol{x}) = (R_{A,i,s,}(t,\boldsymbol{x}), R_{B,i,s}(t,\boldsymbol{x}))$, and $L^T_{i,s}(t,\boldsymbol{x}) = (L_{A,i,s}(t,\boldsymbol{x}), L_{B,i,s}(t,\boldsymbol{x}))$, respectively, where $s =\uparrow,\downarrow$ is the spin index, $i = 1, ..., N$ is the collective index for layer/internal degrees of freedom, and A/B corresponds to the sub-lattice (SL) index. The Hamiltonians for the right- and left- handed fermions are

$$H_R = -iv_f \boldsymbol{\tau} \cdot \boldsymbol{\nabla},\ H_L = \tau_2 H_R \tau_2, \tag{1}$$

where $\boldsymbol{\nabla} = (\partial_1, \partial_2)$ is the two-dimensional gradient operator, and the 2×2 identity matrix τ_0 and the Pauli matrices τ_j's with $j = 1, 2, 3$ act on the sub-lattice (SL) index. We can absorb the Fermi velocity v_F on the imaginary time to write $x_0 = -iv_F t$. Then, after performing the SL transformation $L_{i,s} \to \tau_2 L_{i,s}$ and combining all degrees of freedom into an $8N$-component spinor $\psi^\dagger_{8N} = (R^\dagger_{1,\uparrow}, R^\dagger_{1,\downarrow}, ..., R^\dagger_{2N,\uparrow}, R^\dagger_{2N,\downarrow}, L^\dagger_{1,\uparrow}, L^\dagger_{1\downarrow}, ..., L^\dagger_{2N,\uparrow}, L^\dagger_{2N\downarrow})$, the Euclidean action of $4N$ flavors of Weyl fermions can be written in a manifestly flavor-symmetric form

$$S_0 = \int d^3x\ \bar{\psi}_{8N}\ \mathbb{1}_{4N\times 4N} \otimes \left[\sum_{\nu=0}^{2} \gamma_\nu\ \partial_\nu\right]\ \psi_{8N}, \tag{2}$$

where $\mathbb{1}_{4N\times 4N}$ is the $4N \times 4N$ identity matrix, $\bar{\psi}_{8N} = \psi^\dagger_{8N}\mathbb{1}_{4N\times 4N} \otimes \gamma_0$, $\gamma_0 = \tau_3$, $\gamma_1 = \tau_2$, $\gamma_2 = -\tau_1$. Notice in the Euclidean frequency-momentum space, the Weyl points appear as the unit strength, hedgehog singularities.

The action is invariant under (i) the global $U(1)$ transformation: $\psi_{8N} \to \exp[i\theta\ \mathbb{1}_{4N\times 4N} \otimes \tau_0]\psi_{8N}$, and (ii) the global, flavor symmetry transformation: $\psi_{8N} \to U\psi_{8N}$, with $U \in SU(4N)$. Hence, the free fermion action possesses $U(1) \times SU(4N) = U(4N)$ symmetry, and we can define the conserved total number current $J^0_\mu = \bar{\psi}_{8N}\mathbb{1}_{4N\times 4N} \otimes \gamma_\mu\psi_{8N}$, and the flavor currents $J^i_\mu = \bar{\psi}_{8N}\hat{\Lambda}_i \otimes \gamma_\mu\psi_{8N}$, where $\hat{\Lambda}_i$ with $i = 1, 2, .., (4N)^2 - 1$ are the $4N \times 4N$, Hermitian generators of $SU(4N)$ group. For the $N = 1$ model of spinful mono-layer graphene (MLG), QFH order can describe the QSH or the quantum valley Hall (QVH) states. The $N = 2$ model corresponds to the simplest low energy theory of nearly-flat bands of TBLG.[54–57] For TBLG, the QFH mass can correspond to the QSH, the QVH, or the quantum mini-valley Hall (QMVH) states. Additional Weyl points can also arise from the effects of trigonal warping.[58] The $SU(4N)$ generators can be expressed as suitable linear combinations of direct products of $\log_2(4N)$ sets of identity and Pauli matrices operating on spin and valley type degrees of freedom. While describing MLG and TBLG, we will reserve σ_λ, η_λ, ρ_λ respectively for the spin, the valley (L vs.

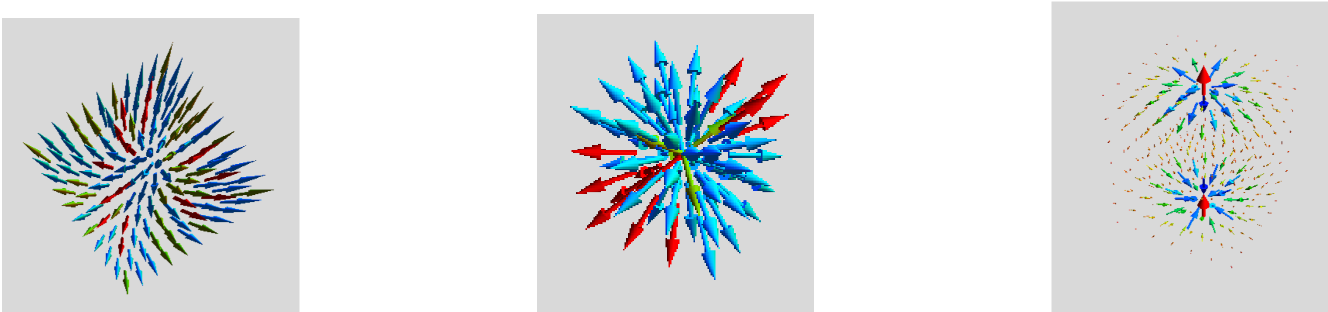

FIG. 1: Illustrations of (a) static skyrmion textures in two-dimensional space with $W_{sk} = -1$ [see Eq. 3], (b) radial hedgehog singularity in (2+1)-dimensional Euclidean space-time with topological invariant $q = +1$ [see Eq. 7], and (c) a dipole configuration due to a pair of hedgehog singularities in (2+1)-dimensional Euclidean space-time with $q_h = \pm 1$. If the hedgehogs are separated along the imaginary time axis, all spatial planes, lying between (outside) the hedgehogs, will (not) exhibit skyrmion textures. Such planes possess "magnetic flux" of unit vector field $\hat{\mathbf{\Omega}}$, obtained by integrating the skyrmion number density J_0^{sk}. If the hedgehogs are separated along any spatial direction, the orthogonal space-time planes will display skyrmion textures. Such planes support "electric flux" of $\hat{\mathbf{\Omega}}$, obtained by integrating the spatial components of skyrmion current density J_i^{sk}, with $i = 1, 2$.

R), and the mini-valley (R_1 vs R_2 within a Moiŕe Brillouin zone) sectors. Individually, each set of Pauli matrices represents an $SU(2)$ sub-group of $SU(4N)$. Next, we consider the skyrmion textures of QFH orders that breaks the corresponding $SU(2)$ sub-group and reduces the symmetry from $SU(4N)$ to $SU(2N) \times U(1)$.

III. SKYRMIONS OF QFH ORDERS

The $SU(2)_s$ symmetry breaking and $SU(2N)$ symmetry preserving, QSH mass term is given by $\mathcal{O}_{QSH} = \mathbf{\Omega}(x) \cdot \bar{\psi} \mathbb{1}_{2N\times 2N} \otimes \boldsymbol{\sigma} \otimes \tau_0 \psi$, where $\mathbf{\Omega}(x)$ is a three-component, vector field. A uniform order parameter field determines a global spin quantization axis along $\mathbf{\Omega} = \mathbf{\Omega}_0$ and the total $U(1)$ spin-current $J^s_\mu = \hat{\mathbf{\Omega}}_0 \cdot \bar{\psi} \mathbb{1}_{2N\times 2N} \otimes \boldsymbol{\sigma} \otimes \gamma_\mu \psi$. In response to the externally applied electro-magnetic and spin gauge fields, the QSH phase supports cross-correlated, charge and spin Hall currents, $J^0_\alpha = \frac{\sigma^s_{xy}}{2\pi}\ \epsilon_{\alpha\mu\nu} F^0_{\mu\nu}$, and $J^s_\alpha = \frac{\sigma^s_{xy}}{2\pi}\ \epsilon_{\alpha\mu\nu} F^s_{\mu\nu}$ where $\sigma^s_{xy} = 2N$ is the quantized spin-Hall conductivity, and the Abelian field strength tensors are $F^i_{\mu\nu} = \partial_\mu A^i_\nu - \partial_\nu A^i_\mu$. Similar results for the cross-correlated charge and flavor quantum Hall currents can be obtained for QVH and QMVH mass orders in TBLG, respectively defined as $\mathcal{O}_{QVH} = \mathbf{\Omega}(x) \cdot \bar{\psi} \boldsymbol{\eta} \otimes \rho_0 \otimes \sigma_0 \otimes \tau_0 \psi$, and $\mathcal{O}_{QMVH} = \mathbf{\Omega}(x) \cdot \bar{\psi} \eta_0 \otimes \boldsymbol{\rho} \otimes \sigma_0 \otimes \tau_0 \psi$.

The smooth, static skyrmion textures of QSH order parameter are described by

$$\hat{\mathbf{\Omega}}(\rho, \varphi) = \Big(\sin[\theta_n(\rho)] \cos(n\varphi), \sin[\theta_n(\rho)] \sin(n\varphi), \cos[\theta_n(\rho)] \Big), \tag{3}$$

where $\varphi = \tan^{-1}(x_2/x_1)$, and $\theta_n(\rho)$ is an interpolating function of the radial variable $\rho = \sqrt{x_1^2 + x_2^2}$, such that $\theta_n(\rho \to 0) \to 0$ and $\theta_n(\rho \to \infty) \to \pi$, with $n = \pm 1, \pm 2, ...$ For any fixed n, the choice of interpolating function $\theta_n(\rho \to 0) \to \pi$ and $\theta_n(\rho \to \infty) \to 0$ changes the sign of skyrmion's winding number, defined by

$$W_{sk} = \frac{n}{2}(\cos[\theta_n(0)] - \cos[\theta_n(\infty)]). \tag{4}$$

The Belavin-Polyakov solutions of unit skyrmions,[59] which minimize the energy of static NLSMs, correspond to

$$\cos(\theta) = \pm \frac{R^{2|n|} - \rho^{2|n|}}{R^{2|n|} + \rho^{2|n|}}, \tag{5}$$

where R is the size of skyrmion core. In Fig. 1(a), we have illustrated the unit skyrmion textures with $W_{sk} = -1$, by using dimensionless coordinates ρ/R, $n = +1$, and $\cos(\theta) = -(R^2 - \rho^2)/(R^2 + \rho^2)$.

Deep inside the ordered phase, the induced fermion current can be computed by employing the gradient expansion scheme, which is controlled by the amplitude $|\mathbf{\Omega}|$. The spin-singlet, total number current is found to be

$$J^0_\mu = \sigma^s_{xy} J^{sk}_\mu = 2N J^{sk}_\mu, \tag{6}$$

where $J^{sk}_\mu = \frac{1}{4\pi}\ \epsilon_{\mu\nu\lambda} \hat{\mathbf{\Omega}} \cdot (\partial_\nu \hat{\mathbf{\Omega}} \times \partial_\lambda \hat{\mathbf{\Omega}})$ is the skyrmion current density. Since the ordered phase does not allow singular tunneling events or hedgehog configurations, both J^{sk}_μ and J^0_μ satisfy the continuity equation. Hence, the induced fermion number $\langle \bar{\psi} \gamma_0 \psi \rangle = 2N \int d^2x J^{sk}_0 = 2N\ W_{sk}$, is determined by the quantized, spin Hall conductivity, and W_{sk} acts as the generator of flavor-singlet,

$U(1)$ symmetry.

As the $SU(2N)$ flavor symmetry remains unbroken, the spin-singlet $SU(2N)$ flavor currents $J^{0,l}_\mu = \bar{\psi}\hat{\lambda}_l \otimes \sigma_0 \otimes \gamma_\mu \psi$, with $l = 1, .., (2N)^2 - 1$ remain identically conserved. When the QSH order is destroyed, the $SU(2)_s$ symmetry is restored, and the condensation of skyrmions is expected to give rise to a spin-singlet, paired state, breaking global $U(1)$ symmetry. Similarly, the valley-(mini-valley-) singlet paired states can arise from the quantum-disordered QVH (QMVH) phase. *However, charge $2e^-$ fermion bilinears break $SU(2N)$ flavor symmetry, when $N > 1$* (see Section V). *Can the skyrmion condensation determine the pattern of flavor-symmetry-breaking (FSB) by paired states*? To answer this question, we consider the role of hedgehog configurations, which serve as the source and sink of J^{sk}_μ.

IV. HEDGEHOGS AND FERMION ZERO MODES

The tunneling singularities in *Euclidean space-time* are also classified according to the second homotopy group $\Pi_2(S^2) = \mathbb{Z}$. The topological invariant or hedgehog charge is given by

$$q = \frac{1}{8\pi} \int d^2 S_a \epsilon_{abc} \, \epsilon_{\alpha\beta\lambda} \, \hat{\Omega}_\alpha \partial_b \hat{\Omega}_\beta \partial_c \hat{\Omega}_\lambda, \tag{7}$$

where the integrals are performed over a sphere surrounding the singularity.[60] The minimal or unit strength ($q = \pm 1$), radial (anti-)hedgehog configurations correspond to $\hat{\Omega}_\mu = \pm \hat{x}_\mu$, i.e.,

$$\hat{\mathbf{\Omega}} = \left[\frac{\rho}{\sqrt{\rho^2 + x_0^2}} \cos\varphi, \frac{\rho}{\sqrt{\rho^2 + x_0^2}} \sin\varphi, \frac{x_0}{\sqrt{\rho^2 + x_0^2}} \right]. \tag{8}$$

In Fig. 1(b), we have illustrated $\hat{\mathbf{\Omega}}_\mu = \hat{x}_\mu$ with $q = +1$. More general hedgehogs with charge $q_h = l$ can be described by

$$\mathbf{\Omega} = \left[F_{1,l}(\rho)\cos(l\varphi), F_{1,l}(\rho)\sin(l\varphi), F_{2,l}(x_0) \right], \tag{9}$$

where $F_{1,l}$ and $F_{2,l}$ are two profile functions with the asymptotic properties: (i) $F_{1,l}(\rho \to 0) \sim \rho^l$, and $F_{1,l}(\rho \to \infty) \sim c_1$, and (ii) $F_{2,l}(x_0 \to 0) \sim x_0$ and $F_{2,l}(x_0 \to \pm\infty) \sim \pm c_2$, with c_1 and c_2 being two constants. By normalizing the vector field in Eqn. 9 we obtain the unit vector field:

$$\hat{\mathbf{\Omega}}(x_0, \rho, \varphi) = \Big(\sin[\theta_l(x_0, \rho)] \cos(l\varphi), \sin[\theta_l(x_0, \rho)] \sin(l\varphi), \cos[\theta_l(x_0, \rho)] \Big), \tag{10}$$

with $\cos[\theta_l(x_0, \rho)] = \frac{F_{2,l}(x_0)}{\sqrt{F^2_{1,l}(\rho) + F^2_{2,l}(x_0)}}$. By rotating these configurations by an angle ϕ about any arbitrary constant unit vector $\hat{\mathbf{n}}$, we can construct various topologically equivalent, hedgehog configurations $\hat{\mathbf{\Omega}}' = \mathcal{R}(\hat{\mathbf{n}}, \phi)\hat{\mathbf{x}}$. where $\mathcal{R}(\hat{\mathbf{n}}, \phi)$ is a 3×3 rotation matrix.

To elucidate the relationship between skyrmions and hedgehogs, we have also illustrated in Fig. 1(c) the dipole configuration of unit vector field due to a pair of hedgehogs with opposite charges $q = \pm 1$. We have used

$$\begin{aligned} \hat{\mathbf{\Omega}} &= \left[\sin\theta_1 \cos(\varphi), \sin\theta_1 \sin(\varphi), \cos\theta_1 \right], \\ \cos[\theta_1(x_0, \rho)] &= \frac{x_0^2 + \rho^2 - R^2}{\sqrt{(x_0^2 + \rho^2 - R^2)^2 + 4\rho^2}}, \end{aligned} \tag{11}$$

and dimensionless space-time coordinates x_μ / R. The hedgehogs, occurring at $x_\mu = (0, 0, \pm R)$, are separated along the imaginary time axis. All spatial planes with $|x_0| < R$ exhibit skyrmion textures with core radius $\sqrt{R^2 - x_0^2}$ and $W_{sk} = +1$. The spatial planes with $|x_0| > R$ do not support any skyrmion textures. Consequently, at the locations of hedgehogs, the skyrmion number jumps by ± 1. If we rather consider a dipole configuration with hedgehogs separated along the spatial x_1-axis, the $x_0 - x_2$ planes will display skyrmion textures. The skyrmions textures for spatial (space-time) planes lead to the quantized magnetic (electric) flux of $\hat{\mathbf{\Omega}}$. For $x_\mu - x_\nu$ planes, the flux is

$$\Phi_{\mu\nu} = \int dx_\mu dx_\nu \, F_{\mu\nu} = 2\pi \, \epsilon_{\lambda\mu\nu} \int dx_\mu dx_\nu \, J^{sk}_\lambda. \tag{12}$$

Due to the non-conservation of skyrmion currents, the continuity equation for the total number current must be modified to

$$\partial_\mu J^0_\mu = 2N \sum_i \, \delta^3(x - x_i) q_i. \tag{13}$$

To satisfy the overall neutrality condition (i.e., $\sum_i q_i = 0$), we must have an equal number of hedgehogs and anti-hedgehogs. A fully self-consistent treatment of fermion-hedgehog interactions lies beyond the scope of current work and we will only discuss the topological structure of fermion propagator or functional determinant in the presence of fixed hedgehog configurations.

Let us consider the coupling between hedgehogs of QSH order parameter and one species of four-component Weyl fermions with sub-lattice and spin index. Due to the $SU(2N)$ flavor symmetry, the results for all species of Weyl fermions will be identical. To facilitate our analysis of fermion-hedgehog scattering and induced pairing, we introduce the Nambu spinor $\Psi^T_N = (\psi^T, \bar{\psi}\gamma_1 \otimes \sigma_2)/\sqrt{2}$ and $\bar{\Psi}_N = (\psi^T \gamma_1 \otimes \sigma_2, \bar{\psi})/\sqrt{2}$, leading to

$$S = \int d^3x \, \bar{\Psi}_N \mathcal{D}_N \Psi_N = \int d^3x \, \bar{\Psi}_N \begin{pmatrix} 0 & \mathcal{D}^\dagger \\ \mathcal{D} & 0 \end{pmatrix} \Psi_N, \tag{14}$$

where $\mathcal{D} = \gamma_\nu \partial_\nu + \boldsymbol{\sigma} \cdot \mathbf{\Omega}$. In this basis, all charge $2e^-$, fermion bilinears will be block diagonal operators. While $\mathcal{D}$ and $\mathcal{D}^\dagger$ are not Hermitian or anti-Hermitian operators,

$\mathcal{D}_N$ is an Hermitian operator. Therefore, the fermion fields Ψ_N and $\bar{\Psi}_N$ can be expanded in the eigenbasis of $\mathcal{D}_N$. The eigenvalues follow from the squared operator

$$\mathcal{D}_N^2 = \begin{pmatrix} \mathcal{D}^\dagger \mathcal{D} & 0 \\ 0 & \mathcal{D}\mathcal{D}^\dagger \end{pmatrix}. \tag{15}$$

Since $\{\mathcal{D}_N, \alpha_3\} = 0$, where α_3 is the diagonal Pauli matrix, operating on the particle-hole index, the non-zero eigenvalues of $\mathcal{D}_N$ come in pairs.

The zero-modes possess definite chirality, corresponding to $\alpha_3 = +1$ (right/annihilation channel) or -1 (left/creation channel). The four-component, right zero-mode ϕ_R (column vector) satisfies $\mathcal{D}\phi_R = \mathcal{D}^\dagger\mathcal{D}\phi_R = 0$ and the four-component, left zero-mode ϕ_L (row vector) obeys $\mathcal{D}^\dagger\phi_L^\dagger = \mathcal{D}\mathcal{D}^\dagger\phi_L^\dagger = 0$. The difference between the number of right zero-modes n_R and the number of left zero-modes n_L is always -$|l|$ for hedgehogs and +$|l|$ for anti-hedgehogs. This result is protected by Callias's index theorem.[61–63]

For the unit-strength, radial (anti-)hedgehog configurations, with $\boldsymbol{\Omega}_\mu = \pm\, m(x)\ \hat{x}_\mu$, where m is amplitude of the order parameter, the zero-mode eigenfunctions are given by

$$\phi^*_{+,L} = \phi^T_{-,R} = (0, 1, -i, 0) f(|x|), \tag{16}$$

where $f(|x|) \propto \exp\left[-\int dx' m(x')\right]$. For a constant m, we obtain $f(|x|) = \sqrt{\frac{|m|^3}{2\pi}} e^{-m|x|}$.[17] In this case, one can also determine the full spectra of $\mathcal{D}$ by following Refs. 61,62. The bound states of $\mathcal{D}_N$ have eigenvalues

$$\lambda_n = \pm m\, \sqrt{1 - n^{-2}}, \tag{17}$$

with $n = 1, 2, ..$, and they exhibit $2N \times n^2$-fold degeneracy.

After accounting for the $2N$-fold degeneracy in flavor index, we find that the total number of topologically protected fermion zero-modes is equal to $\sigma^f_{xy} \times |l| = 2N|l|$. This is a highly non-trivial result, as the quantum-disordered state does not support long-range quantum flavor Hall order. In the absence of adiabatic control provided by the long-range order, only the direct calculations of fermion zero modes of dynamic Weyl operator can unambiguously demonstrate the breakdown of fermion number conservation law.

The effective action of isolated hedgehogs due to the coupling with fermion fields is determined by $\mathrm{Tr}[\log(G^{-1})] = \log[\det(G^{-1})]$, where the inverse propagator of fermion fields $G^{-1} = \mathcal{D}_N$. The functional determinant $\det(G^{-1}) = \det(\mathcal{D}_N)$ is also known as the fermion determinant (or Pfaffian). The existence of zero-modes for the dynamic Weyl operator $\mathcal{D}_N$ indicates the fermion determinant vanishes in the presence of isolated hedgehogs and hence the effective action of hedgehogs displays logarithmic, infra-red divergence. This signals instability toward competing mass order generation, which we outline in the next section.

V. PAIRING BILINEARS

In this section, we identify charge $2e^-$ *pairing mass terms* which anti-commute with both the Hamiltonian and QFH mass terms, and cause superconducting gaps for the Weyl fermions. Since the zero-mode expectation values for all particle-hole bilinears vanish identically, only charge $2e^-$ pairing mass operators can possess non-vanishing expectation values from zero-mode eigenfunctions, and are capable of curing the instability of the vacuum, arising from the vanishing of the fermion determinant (or the logarithmic divergence of action). Using the examples of MLG ($N = 1$) and TBLG ($N = 2$), we will also elucidate the relationship with appropriate $SO(5)$ and $SO(9)$ NLSMs of competing orders as well as WZW terms.

For the general case of $4N$-flavors of Weyl fermions, all momentum-independent, charge $2e^-$ pairing terms can be described as $\phi_{l,1}\Psi^\dagger\alpha_1\hat{\Lambda}'_l\Psi$ and $\phi_{l,2}\Psi^\dagger\alpha_2\hat{\Lambda}'_l\Psi$, where $\Psi^\dagger = (\psi^\dagger, \psi^T)/\sqrt{2}$ is the $16N$-component Nambu spinor, $\hat{\Lambda}'_l$ are the $4N(8N-1)$ number of $8N \times 8N$, imaginary, $SU(8N)$ Gell-Mann matrices, and the Pauli matrices α_j's operate on the particle-hole index. Notice that the number of pairing bilinears $4N(8N-1)$ exactly equals the number of generators for $SO(8N)$ group. Out of these bilinears, only $\Psi^\dagger\alpha_j \otimes \hat{M} \otimes \tau_2\Psi$, with symmetric $4N \times 4N$ matrix $\hat{M}$ can anti-commute with the Hamiltonian of free fermions and act as superconducting mass terms. There are $2N(4N+1)$ independent, charge $2e^-$, mass terms, which is equal to the number of generators for $USp(4N)$ group. By absorbing the imaginary Pauli matrices (η_2, ρ_2 etc.) from all $SU(2)$ sectors on the lower component of Nambu spinor, the pairing mass terms can be organized in a more convenient singlet and triplet forms.

A. MLG

For MLG with $N = 1$, we will absorb $\eta_2 \otimes \sigma_2 \otimes \gamma_1$ into the lower component of Nambu spinor: $\Psi_1^T = (\psi_1, \tilde{\psi}_1^*)^T/\sqrt{2} = (\psi_1, \eta_2 \otimes \sigma_2 \otimes \gamma_1 \bar{\psi}_1^T)^T/\sqrt{2}$, and define the barred Nambu spinor with an additional α_1 absorbed: $\bar{\Psi}_1 = \alpha_1(\bar{\psi}_1, \tilde{\psi}_1^T)/\sqrt{2} = (\psi_1^T\eta_2 \otimes \sigma_2 \otimes \gamma_1, \bar{\psi}_1)/\sqrt{2}$. In this basis, the QSH and QVH mass terms become

$$\mathcal{O}_{QSH} = \boldsymbol{\Omega}_1 \cdot \bar{\Psi}\alpha_1\alpha_3 \otimes \eta_0 \otimes \boldsymbol{\sigma} \otimes \tau_0\Psi, \tag{18}$$

$$\mathcal{O}_{QVH} = \boldsymbol{\Omega}_2 \cdot \bar{\Psi}\alpha_1\alpha_3 \otimes \boldsymbol{\eta} \otimes \sigma_0 \otimes \tau_0\Psi, \tag{19}$$

while the Hamiltonian operator of free fermion acquires the form $H_f = \sum_{j=1}^2\ \bar{\Psi}\alpha_1\alpha_3 \otimes \mathbb{1}_{4\times4} \otimes \gamma_j\partial_j\Psi$. The ten possible pairing masses can be rewritten as

$$\mathcal{O}_{s,j} = \phi_{s,j}\bar{\Psi}\alpha_1\alpha_j \otimes \eta_0 \otimes \sigma_0 \otimes \tau_0\Psi, \tag{20}$$

$$\mathcal{O}^{mn}_{t,j} = \phi^{mn}_{t,j}\bar{\Psi}\alpha_1\alpha_j \otimes \eta_m \otimes \sigma_n \otimes \tau_0\Psi, \tag{21}$$

with m and n being equal to $1, 2, 3$. Only the spin and valley singlet, s-wave, pairing mass $\mathcal{O}_{s,j}$ can anti-commute with H_f, $\mathcal{O}_{QSH}$ and $\mathcal{O}_{QVH}$. Hence, the condensation of skyrmion textures of both QSH and QVH order parameters in the para-magnetic phase can lead to a unique, charge $2e^-$, spin- and valley- singlet, s-wave pairing mass. This pairing mass order will shift the zero mode spectrum and lead to non-zero fermion determinant. This can be seen by considering $\mathcal{O}_{s,1} = \phi_{s,1}\bar{\Psi}\alpha_0 \otimes \eta_0 \otimes \sigma_0 \otimes \tau_0 \Psi$ with constant amplitude $\phi_{s,1}$ and hedgehog order parameter. In this case, both zero modes will obtain a finite energy eigenvalue $\phi_{s,1}$. Consequently, the fermion determinant will receive a factor of $\phi_{s,1}^2$. Hence, the fermion determinant will no longer vanish and the instability of the ground state or vacuum is cured by forming a superconducting condensate.

From the pairing mass orders, we can consequently construct two quintuples

$$\mathbf{N}_1 = (\Omega_{1,1}, \Omega_{1,2}, \Omega_{1,3}, \phi_{s,1}, \phi_{s,2}), \tag{22}$$
$$\mathbf{N}_2 = (\Omega_{2,1}, \Omega_{2,2}, \Omega_{2,3}, \phi_{s,1}, \phi_{s,2}), \tag{23}$$

for describing competition between particle-hole and particle-particle channels. Simple matrix algebra shows the resulting $SO(5)$ NLSMs support level-1 WZW term. Since the pairing mass orders are valley singlets and hence preserve the flavor symmetry of MLG, it is expected that the effective pairing vertex should be a charge $2e^-$ bilinear. We will show in the next section that this is indeed the case. [see Eq. (38)]. Since the spin and valley triplet pairing mass terms $\mathcal{O}^{mn}_{t,j}$ do not anti-commute with $\mathcal{O}_{QSH}$ or $\mathcal{O}_{QVH}$, they are not favored as emergent, pairing orders.

B. TBLG

For TBLG with $N = 2$, we absorb $\eta_2 \otimes \rho_2 \otimes \sigma_2 \otimes \gamma_1$ into the lower component of Nambu spinor: $\Psi_2^T = (\psi_2, \tilde{\psi}_2^*)^T/\sqrt{2} = (\psi_2, \eta_2 \otimes \rho_2 \otimes \sigma_2 \otimes \gamma_1 \bar{\psi}_2^T)^T/\sqrt{2}$, and define the barred Nambu spinor with an additional α_1 absorbed: $\bar{\Psi}_2 = \alpha_1(\bar{\psi}_2, \tilde{\psi}_2^T)/\sqrt{2} = (\psi_2^T \eta_2 \otimes \rho_2 \otimes \sigma_2 \otimes \gamma_1, \bar{\psi}_2)/\sqrt{2}$. In this basis, the QSH, QVH, QMVH mass terms become

$$\mathcal{O}_{QSH} = \mathbf{\Omega}_1 \cdot \bar{\Psi}\alpha_1\alpha_3 \otimes \eta_0 \otimes \rho_0 \otimes \tau_0 \otimes \boldsymbol{\sigma}\Psi, \tag{24}$$
$$\mathcal{O}_{QVH} = \mathbf{\Omega}_2 \cdot \bar{\Psi}\alpha_1\alpha_3 \otimes \boldsymbol{\eta} \otimes \rho_0 \otimes \tau_0 \otimes \sigma_0\Psi, \tag{25}$$
$$\mathcal{O}_{QMVH} = \mathbf{\Omega}_3 \cdot \bar{\Psi}\alpha_1\alpha_3 \otimes \eta_0 \otimes \boldsymbol{\rho} \otimes \tau_0 \otimes \sigma_0\Psi, \tag{26}$$

while the Hamiltonian operator of free fermion acquires the form $H_f = \sum_{j=1}^2 \bar{\Psi}\alpha_1\alpha_3 \otimes \mathbb{1}_{8\times8} \otimes \gamma_j \partial_j \Psi$. The pairing mass terms can be grouped into four categories:

$$\mathcal{O}^{00l}_{st,j} = \phi^{00l}_{st,j}\bar{\Psi}\alpha_1\alpha_j \otimes \eta_0 \otimes \rho_0 \otimes \sigma_l \otimes \tau_0\Psi, \tag{27}$$
$$\mathcal{O}^{l00}_{vt,j} = \phi^{l00}_{vt,j}\bar{\Psi}\alpha_1\alpha_j \otimes \eta_l \otimes \rho_0 \otimes \sigma_0 \otimes \tau_0\Psi, \tag{28}$$
$$\mathcal{O}^{0l0}_{mt,j} = \phi^{0l0}_{mt,j}\bar{\Psi}\alpha_1\alpha_j \otimes \eta_0 \otimes \rho_l \otimes \sigma_0 \otimes \tau_0\Psi, \tag{29}$$
$$\mathcal{O}^{lmn}_{at,j} = \phi^{lmn}_{at,j}\bar{\Psi}\alpha_1\alpha_j \otimes \eta_l \otimes \rho_m \otimes \sigma_n \otimes \tau_0\Psi, \tag{30}$$

where l, m, and n can take values $1, 2, 3$. They respectively describe pairing bilinears, which are spin-triplet, valley-triplet, mini-valley-triplet, and triplets in all flavor channels. The physical significance of relevant pairing mass terms are described in Table I.

The QSH mass for $N = 2$ model anti-commutes with charge $2e^-$ bilinears $\mathcal{O}^{l00}_{vt}$ and $\mathcal{O}^{0l0}_{mt}$. Similar to MLG, each of the TBLG pairing bilinears will by itself contribute a factor of $(\phi^{l00}_{vt,j})^4$ or $(\phi^{0l0}_{mt,j})^4$ to the fermion determinant and hence cure the instability. However, any of the valley(mini-valley)-triplet bilinears $\mathcal{O}^{l00}_{vt}$ ($\mathcal{O}^{0l0}_{mt}$) by itself will lead to two zero modes obtaining positive eigenvalues and the other two zero modes obtaining negative eigenvalues, which explicitly breaks $SU(4)$ flavor symmetry in the valley (mini-valley) sector. Hence, the effective pairing vertex cannot be in the form of charge $2e^-$ bilinears and must be a four-fermion term that preserves the $SU(4)$ flavor symmetry. We will construct this pairing vertex in the next section.

From the pairing mass orders in TBLG, there are six possible ways to form *quintuples*

$$\mathbf{N}_1^l = (\Omega_{1,1}, \Omega_{1,2}, \Omega_{1,3}, \phi^{l00}_{vt,1}, \phi^{l00}_{vt,2}), \tag{31}$$
$$\mathbf{N}_2^l = (\Omega_{1,1}, \Omega_{1,2}, \Omega_{1,3}, \phi^{0l0}_{mt,1}, \phi^{0l0}_{mt,2}), \tag{32}$$

with $l = 1, 2, 3$, and all six types of $SO(5)$ NLSMs will support level-2 WZW term. Again, due to the presence of multiple pairing mass terms, the skyrmion condensation cannot select any specific charge $2e^-$ pairing channel, without any additional mechanism of breaking $SU(4)$ flavor symmetry.

It is possible to combine all competing mass terms into a *nonuple*

$$\mathbf{L} = (\Omega_1, \Omega_2, \Omega_3, \phi^{100}_{vt,1}, \phi^{200}_{vt,1}, \phi^{300}_{vt,1}, \phi^{010}_{mt,2}, \phi^{020}_{mt,2}, \phi^{030}_{mt,2}), \tag{33}$$

and write down $SO(9)$ NLSM for $\hat{\mathbf{L}}$. The $SO(9)$ NLSM treats all mutually anti-commuting mass orders on an equal footing. The resulting coset space $SO(9)/SO(8)$ is closely tied to the octonion gauge theories and details of such exotic aspects will be provided elsewhere. Within the $SO(9)$ model, the pairing mass terms are embedded as a *sextuple*. The appearance of $SO(6)$ is a natural consequence of $SU(4)$ being the double cover of $SO(6)$. Similar results can be obtained for the combinations $(\mathcal{O}_{QVH}, \mathcal{O}^{00l}_{st,j}, \mathcal{O}^{0l0}_{mt,j})$ and $(\mathcal{O}_{QMVH}, \mathcal{O}^{l00}_{vt,j}, \mathcal{O}^{00l}_{st,j})$, as shown in Table I. This type of *triality* is a consequence of the underlying $SU(8)$ flavor symmetry.

In Table I, we also identify the irreducible representation of pairing mass terms under the discrete symmetry operations of point group D_6[45]. For our Nambu spinors Ψ and $\bar{\Psi}$, we have defined the following operations:

$$C_3: \quad k_\pm \to e^{\pm i\frac{2\pi}{3}}k_\pm,\ \Psi \to e^{-i\frac{2\pi}{3}\gamma_0}\Psi, \bar{\Psi} \to \bar{\Psi}e^{i\frac{2\pi}{3}\gamma_0}, \tag{34}$$

$$C_{2x}: \quad k_x \to k_x,\ k_y \to -k_y,\ \Psi \to \alpha_0\eta_3\rho_1\gamma_2\Psi, \quad \bar{\Psi} \to -\bar{\Psi}\alpha_0\eta_3\rho_1\gamma_2, \tag{35}$$

Charge $2e^-$ pairing operators	Anti-commuting QFH orders	Physical significance
$\mathcal{O}^{l00}_{vt,j}$	QMVH, QSH	$\mathcal{O}^{100}_{vt,j}$: spin-singlet, A_1, PDW pairing; (C_3^+, C_{2x}^+, C_{2y}^+, C_2^+) $\mathcal{O}^{200}_{vt,j}$: spin-singlet, B_1, PDW pairing; (C_3^+, C_{2x}^+, C_{2y}^-, C_2^-) $\mathcal{O}^{300}_{vt,j}$: spin-singlet, A_2, BCS pairing; (C_3^+, C_{2x}^-, C_{2y}^-, C_2^+)
$\mathcal{O}^{0l0}_{mt,j}$	QVH, QSH	$\mathcal{O}^{010}_{mt,j}$: spin-singlet, B_2, MPDW pairing; (C_3^+, C_{2x}^-, C_{2y}^+, C_2^-) $\mathcal{O}^{020}_{mt,j}$: spin-singlet, A_1, MPDW pairing; (C_3^+, C_{2x}^+, C_{2y}^+, C_2^+) $\mathcal{O}^{030}_{mt,j}$: spin-singlet, A_1, BCS pairing; ; (C_3^+, C_{2x}^+, C_{2y}^+, C_2^+)
$\mathcal{O}^{00l}_{st,j}$	QVH, QMVH	$\mathcal{O}^{00l}_{st,j}$: spin-triplet, B_2, BCS pairing; (C_3^+, C_{2x}^-, C_{2y}^+, C_2^-)

TABLE I: List of pairing mass terms [defined by Eqs. 27-29] that anti-commute with the three types of quantum flavor Hall (QFH) orders [defined by Eqs. 24 - 26] for twisted bilayer-graphene (TBLG with $N = 2$). They describe relevant competing charge $2e^-$ orders of QFH insulators in the vicinity of charge neutrality ($\nu = 0$). The physical significance of pairing mass terms with $j = 1, 2$, and $l = 1, 2, 3$, and the corresponding irreducible representation under point group D_6 are identified. Acronyms used for pairing masses are: PDW – intra-valley, inter-mini-valley, pair-density waves with large center of mass momentum, MPDW – inter-valley, intra-mini-valley, Moiŕe pair-density waves, with small center of mass momentum, and BCS – inter-valley, inter-mini-valley, zero center of mass momentum pairing. All pairing masses in this table preserve three-fold rotation symmetry and C_i^+ (C_i^-) denotes whether a discrete symmetry (C_i) of D_6 point group is preserved (broken) [see Eqs. 34-37]. For each QFH order, there are six competing charge $2e^-$ bilinears, which describe a basis for addressing residual $SO(6) = SU(4)/\mathbb{Z}_2$ flavor symmetry. Since the skyrmion textures of QFH orders do not break flavor symmetry and carries charge $4e^-$, all six pairing bilinears and flavor symmetry preserving charge $4e^-$ pairing will exist inside the skyrmion core as fluctuating orders. With a suitable gauge choice for pairing amplitudes, the six pairing mass terms and the QFH orders can be combined into a nonuple or nine-component vector field for an unbiased description of competing orders, leading to $U(1) \times SO(9) = U(1) \times USp(8)/\mathbb{Z}_2$ non-linear sigma models [see Eq. 33].

$$\begin{aligned} C_{2y}: \quad & k_x \to -k_x,\ k_y \to k_y,\ \Psi \to \alpha_3\eta_1\rho_0\gamma_1\Psi, \\ & \bar{\Psi} \to \bar{\Psi}\alpha_3\eta_1\rho_0\gamma_1, \end{aligned} \tag{36}$$

$$\begin{aligned} C_2: \quad & k_x \to -k_x,\ k_y \to k_y,\ \Psi \to \alpha_3\eta_2\rho_1\gamma_0\Psi, \\ & \bar{\Psi} \to -\bar{\Psi}\alpha_3\eta_2\rho_1\gamma_0, \end{aligned} \tag{37}$$

with $k_\pm = k_x \pm ik_y$. By construction, all pairing mass terms transform as rotational scalars. Based on the transformation properties under C_{2x}, C_{2y}, and C_2, the mass terms will follow A_1, A_2, B_1 and B_2 representations of D_6, as summarized in Table I.

VI. 't HOOFT VERTEX AND PAIRING AT $\nu = 0$

Now we construct the $SU(4N)$ flavor-symmetry-preserving effective TV for MLG and TBLG in the vicinity of quantum phase transitions, where we can consider a dilute gas of hedgehogs due to the divergent correlation length. Therefore, the overlap between widely separated zero-modes provides a clear idea about the nature of competing orders, arising from the condensation of skyrmions.

Since a strength l (anti-)hedgehog leads to $2N|l|$ zero-modes in the (annihilation) creation channel, we anticipate a (anti-)hedgehog creation operator will be coupled to $2N|l|$ number of fermion (annihilation) creation operators. The calculation of such effective TV can be performed by following Refs.[17,51,53] It is crucial to average over the arbitrary orientations of hedgehogs for a disordered or para-magnetic phase. The eigenfunction of arbitrarily oriented and radial hedgehogs are related by $SU(2)$ rotations $\psi(\hat{\boldsymbol{n}}, \phi) = \mathcal{U}^\dagger\psi(\hat{x})$, where $\mathcal{U} = \pm e^{i\phi/2\hat{\boldsymbol{n}}\cdot\boldsymbol{\sigma}}$, such that $\hat{\mathbf{n}}\cdot\boldsymbol{\sigma} = \mathcal{U}^\dagger\hat{x}\cdot\boldsymbol{\sigma}\mathcal{U}$. Since higher-$l$ hedgehogs will have lower probability, we will only consider TV due to $l = \pm1$ hedgehogs.

After performing the integral over $SU(2)$ group, the two-fermion, TV for MLG with $N = 1$ becomes

$$Y = y\int d^3k f^2(k)k^2\epsilon^{ij}[\psi_i^T(-k)\psi_j(k) + \bar{\psi}_i(k)\bar{\psi}_j^T(-k)], \tag{38}$$

where y is the fugacity of $l = \pm1$ hedgehogs, $i, j \in \{R, L\}$, and ψ^T and $\bar{\psi}^T$ have $\gamma_1 \otimes \sigma_2$ absorbed by definition. The form factor $f(k) = \frac{4\sqrt{2\pi}m^{5/2}}{(k^2+m^2)^2}$ is the Fourier transform of $f(r) = \sqrt{\frac{|m|^3}{2\pi}}e^{-|m|r}$. The TV describes *frequency-momentum dependent charge $2e^-$ bilinear in the spin-singlet, s-wave pairing channel.* Due to the exponentially localized behavior of zero-mode eigenfunctions, $f(k)$ exhibits short-ranged behavior. Since the minimal hedgehogs induce charge $2e^-$ pairing mass, the use of level-1 $SO(5)$ WZW theory for describing competing orders is justified. The charge $4e^-$ pairing for MLG is associated with condensation of skyrmions with $W_{sk} = \pm 2$, which can only take place through interactions between fermions and double hedgehogs. However, on a very general ground we expect the fugacity (or probability) of double hedgehogs to be suppressed in comparison with single hedgehogs. Therefore, the charge $2e^-$ ($4e^-$) pairing is (not) a natural candidate for MLG.

For TBLG with $N = 2$, the calculation of quartic TV due to four degenerate zero-modes of minimal hedgehogs requires some algebraic manipulations. The final result is given by

$$\begin{aligned} Y =& y \int d^3k_1 \int d^3k_2 |f(k_1)|^2 |f(k_2)|^2 k_1^2 k_2^2 \\ & \epsilon^{ijkl}[\psi_i^T(-k_1)\psi_j(k_1)\psi_k^T(-k_2)\psi_l(k_2) + h.c.], \end{aligned} \tag{39}$$

where $i, j \in \{R_1, R_2, L_1, L_2\}$ and ψ^T and $\bar{\psi}^T$ have $\gamma_1 \otimes \sigma_2$ absorbed by definition. *The quartic, TV describes spin-singlet, composite, charge* $4e^-$ *paired state that preserves* $SU(4)$ *symmetry in the combined valley and mini-valley space (enforced by* ϵ^{ijkl}*).* Obviously, such a phase cannot be described by fermion bilinears. Similar conclusions can be drawn for the quantum-disordered QVH and QMVH phases. *In summary, hedgehogs only break* $U(1)$ *symmetry and induce pairing, without breaking flavor symmetry.* Therefore, quantum-disordering of all three types of QFH orders at $\nu = 0$ (or in its immediate vicinity) naturally gives rise to the same charge $4e^-$ superconductivity, which preserves full $SU(8)$ flavor symmetry and only breaks $U(1)$ (total number) symmetry down to $\mathbb{Z}_4$.

In order to realize charge $2e^-$ states for $N \geq 2$, the $SU(2N)$ symmetry must be broken spontaneously or through additional mechanism. In contrast to the long-range tail of Coulomb interactions, the generic short-range interactions do not respect flavor symmetry, inherited from the valley/mini-valley degrees of freedom. Thus, the precise nature of charge $2e^-$ ground state will depend on many non-universal details of short-range interactions. For TBLG, the charge $2e^-$ ground state selects one (or a linear combination) out of the six possible pairing mass orders. For quantum disordered QSH phase, this corresponds to a pattern of FSB $SO(6) = \frac{SU(4)}{\mathbb{Z}_2} \to SO(5) = \frac{USp(4)}{\mathbb{Z}_2}$, which leads to five Goldstone modes from the combined valley and mini-valley $SU(4)$ space. In contrast to this, the flavor symmetry preserving charge $4e^-$ state does not lead to Goldstone modes from the $SU(4)$ flavor space. From the stand-point of charge $2e^-$ operators, the charge $4e^-$ state corresponds to the quantum-disordered phase of $SO(6)$ sigma model fields $\mathbf{\Phi} = (\mathbf{\Phi}_{vt,1}, \mathbf{\Phi}_{mt,2})$. In this phase, charge $2e^-$ pairing fields can have non-vanishing amplitude, i.e., $|\mathbf{\Phi}| = \Phi_0$.

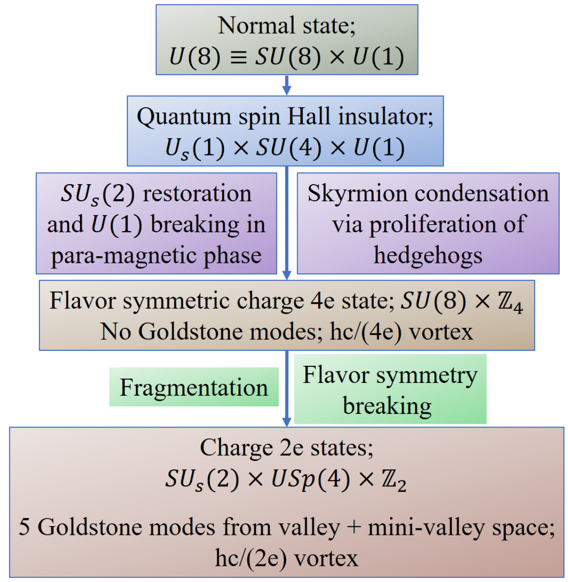

FIG. 2: Summary of the main results for twisted bi-layer graphene (TBLG with $N = 2$), with correlated insulator at $\nu = 0$ being described by the quantum spin Hall (QSH) order. The most favorable paired state at $\nu = 0$ or its immediate vicinity is a $SU(8)$ flavor symmetry preserving charge $4e^-$ phase. Inside the superconducting state, the $SO(6) = SU(4)/\mathbb{Z}_2$ symmetry in the combined valley and mini-valley space can be spontaneously broken down to $SO(5) = USp(4)/\mathbb{Z}_2$, giving rise to charge $2e^-$ BCS, or pair-density-waves, or Moiŕe-pair-density waves [see Table I], and five Goldstone modes. The other two types of quantum flavor Hall orders support the same charge $4e^-$ state. But the fragmentation of $4e^-$ state through spontaneous symmetry breaking will involve charge $2e^-$ spin-singlet and spin-triplet pairings. Whether the charge $4e^-$ or $2e^-$ states are realized can be detected from the presence of $hc/4e$ or $hc/2e$ vortices.

But they do not exhibit global long-range order, i.e.,

$$\langle \mathbf{\Phi}(\boldsymbol{x}_1) \cdot \mathbf{\Phi}(\boldsymbol{x}_2) \rangle \sim e^{-(|\boldsymbol{x}_1 - \boldsymbol{x}_2|)/\xi}, \tag{40}$$

where ξ is the correlation length of charge $2e^-$ pairing fields.

This structure of $SO(6)$ flavor symmetry remains intact even in the presence of finite carrier densities (or a chemical potential E_0). Within a mean-field description, if we consider uniform amplitudes of various components of nonupole $\mathbf{L} = (\mathbf{\Omega}_0, \mathbf{\Phi}_0)$ [see Eq. 33], the fermion spectra will be given by

$$E(\boldsymbol{k}) = \pm[(\sqrt{\boldsymbol{k}^2 + \mathbf{\Omega}_0^2} \pm E_0)^2 + \mathbf{\Phi}_0^2]^{1/2}. \tag{41}$$

where $\pm E_0$ describe the asymmetry between conduction (-) and valence bands (+). At charge neutrality, due to the symmetry between conduction and valence

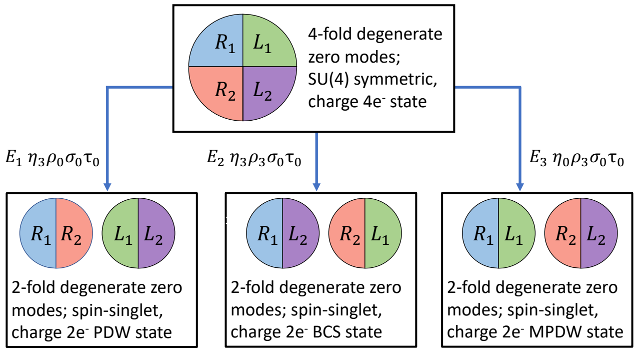

FIG. 3: The degeneracy of fermion zero-modes, localized on hedgehog configurations of quantum spin Hall order parameter and the nature of paired state. Here, E_1, E_2 and E_3 represent three different types of flavor symmetry breaking chemical potentials.

bands the spectral gap at Dirac points is determined by $2|\boldsymbol{L}| = 2\sqrt{\boldsymbol{\Omega}_0^2 + \boldsymbol{\Phi}_0^2}$. Away from the charge neutrality, the spectral gap at the Fermi surfaces from conduction or hole type carriers is controlled by $2|\boldsymbol{\Phi}_0|$. Therefore, the quantum-disordering of $\boldsymbol{\Phi}(\boldsymbol{x})$ and charge $4e^-$ pairing also remain valid for the metallic phase in the vicinity of $\nu = 0$.

For quantum-disordered QVH and QMVH states, we can provide similar arguments. For example, for the quantum-disordered QVH state, the $SO(6)$ vector $\boldsymbol{\Phi}$ constructed from spin-triplet B_2 pairings, spin-singlet A_1 BCS pairing, spin-singlet A_1 and B_2 MPDW pairings (using Table I) captures competition between spin- singlet and triplet pairing channels. When Φ has a non-vanishing amplitude but lacks global long-range order, the same charge $4e^-$ phase is realized. Our main predictions for pairing in the vicinity of $\nu = 0$ are summarized in Fig. 2.

VII. EFFECTS OF FLAVOR-SYMMETRY-BREAKING AT $\nu \neq 0$

The FSB by high-temperature orders can also be instrumental in selecting charge $2e^-$ states in the vicinity of $\nu = \pm 2, \pm 3$. For example, we can consider flavor dependent chemical potentials, which shift various Weyl points to different reference energies. Such chemical potentials couple to the flavor-density operators and reduce the strength of σ^f_{xy} from being $2N$ to N or lower. The experimental data of Refs. 32,33 indeed suggest the presence of FSB chemical potentials, which can cause revival of Weyl points, in the vicinity of Fermi level. For TBLG, in addition to the conventional chemical potential (E_0) for the total number operator, we can consider three types of spin-singlet, chemical potentials (E_j with $j = 1, 2, 3$) in the valley and mini-valley space. When $E_0 = \pm E_j$, the degeneracy of zero-modes is reduced to 2.

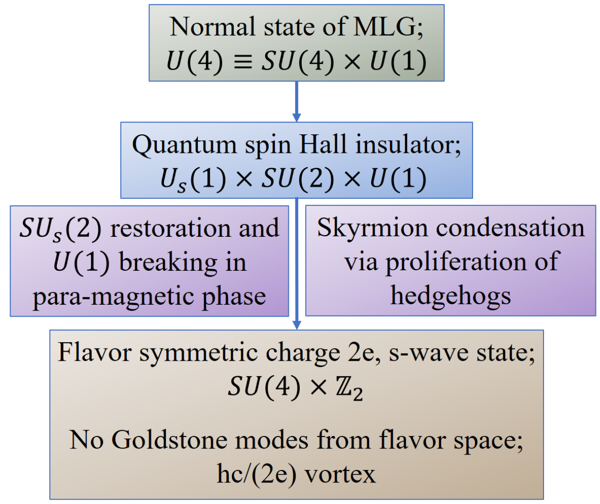

FIG. 4: Summary of the main results for mono-layer graphene (MLG) at charge neutrality and the twisted bi-layer graphene in the vicinity of $\nu = \pm 2, \pm 3$, if the correlated insulating states are described by quantum spin Hall order. The presence of flavor symmetry breaking, high temperature order described by flavor chemical potentials in TBLG give rise to $N = 1$ type low-energy Dirac theories. As discussed in Sec. VII and illustrated in Fig. 3, the form of charge $2e^-$ pairing is determined by the type of flavor chemical potentials. If the correlated insulator is described by quantum valley or mini-valley Hall orders, the charge $2e^-$ spin-triplet BCS type pairing become important.

As illustrated in Fig. 3, depending on the explicit nature of FSB chemical potentials, charge $2e^-$ BCS (zero center of mass momentum), pair-density-waves/PDW (large center of mass momentum or short wavelength modulations), and Moiŕe pair-density-waves/MPDW (small center of mass momentum or long wavelength modulations) states can be realized by destroying QSH order. Very similar considerations for QVH and QMVH orders show the possibilities of realizing spin-singlet and spin-triplet, charge $2e^-$ states in BCS and pair-density-wave channels. Since $SU(4)$ flavor symmetry is already reduced to $SU(2)$ by high-temperature order, the pairing due to skyrmion condensation does not give rise to additional Goldstone modes from flavor space. The situation is similar to the MLG case, which is summarized in Fig. 4.

VIII. OUTLOOK

Our work provides a non-perturbative framework for understanding the competing ground states of TBLG in the vicinity of $\nu = 0$. We have predicted the possibility of realizing charge $4e^-$ pairing in the proximity of charge neutral point due to the condensation of skyrmion textures of QSH, QVH, or QMVH orders. While charge $4e^-$

state shows $SU(8) \times \mathbb{Z}_4$ flavor symmetry, the charge $2e^-$ states exhibit $SU(2) \times USp(4) \times \mathbb{Z}_2$ symmetry. These states can be distinguished by identifying Goldstone modes and performing Josephson junction type experiments. While the genuine two dimensionality of TBLG does not allow for bulk scattering experiments, the collective modes can in principle be identified by studying elastic properties under applied strain. The simplest diagnosis of charge $4e^-$ vs. charge $2e^-$ states by studying the flux quantization rule ($hc/4e$ vs. $hc/2e$ vortices) is within the reach of current experiments.

On the technical front, we have described the mechanism of skyrmion condensation inside the quantum-disordered or para-magnetic phase of non-linear sigma models by studying the interactions between fermions and hedgehogs. The analysis of fermion-hedgehog interactions has not been presented in other closely related works, which have considered topological pairing mechanism for twisted bilayer graphene. In Ref. 45, only two out six competing charge $2e^-$ orders (spin-singlet A_1 and A_2) were identified as potential competing orders of quantum spin Hall phase, and it was suggested that the charge $2e^-$ pairing could occur through condensation of merons (half-skyrmions with winding numbers $W_{sk}/2$). Our analysis shows that the skyrmions (merons) of TBLG will support electric charge $4e^-$ ($2e^-$) and $SO(6)$ structure of flavor symmetry. Thus, the nucleation of charge $2e^-$ paired state must address $SO(6)$ symmetry breaking, irrespective of the meron or the skyrmion condensation. The numerical simulations of microscopic models can provide further guidance on this intriguing issue of proximate, competing orders. But one must be careful with non-universal details of microscopic short range interactions and ungainly details of band-structures.

The structure of flavor symmetry and the mechanism of skyrmion condensation identify dual relationship between particle-hole orders and particle-particle orders. Can such duality be addressed by experiments? There are growing experimental and theoretical evidence in favor of QFH order at various integer filling fractions.[23–35,64–68] However, the precise nature of QFH order for all commensurate filling fractions are still unknown due to the lack of experimental evidence of collective modes. In Ref. 26,27,34, correlated insulating states (except at $\nu = 0$) were suppressed in favor of paired states by using metallic screening layer. Furthermore, the application of small out of plane magnetic field caused reappearance of insulating states. These experiments do emphasize close competition between insulating and superconducting states, which would be consistent with the duality between particle-hole orders and particle-particle orders. The screening of Coulomb interactions is a microscopic tuning mechanism for destroying global long-range order in particle-hole channel. Within our effective theory, the disordering of quantum flavor Hall type order implies the proliferation or condensation of hedgehog type tunneling events. Since the hedgehog creation operator is directly related to the violation of fermion number conservation law, we do anticipate superconductivity.

However, to establish any precise notion of duality, one must address the collective modes which cause rotations between particle-hole and particle-particle orders. Such operators correspond to additional fermion bilinears from pairing channels (non-mass operators). These are the analogs of π-resonance modes in neutron scattering, proposed by Demler *et al.* [69] within the framework of $SO(5)$ theory of competition between spin-triplet, antiferromagnetism and spin-singlet, d-wave superconductivity. For $SO(5)$ theory, the π-modes correspond to spin-triplet pairing operators and the number of such spinful, charged modes is 6. Away from $\nu = 0$, various $SO(5)$ theories of competing particle-hole and pairing orders support similar π-modes. Depending on the details of theories π-modes can be spin-singlet or spin-triplet operators. For TBLG at charge neutrality, the total number of π-modes (say rotating spin-triplet QSH to six, complex, spin-singlet, pairing mass terms) is 36 and they correspond to different types of spin-triplet pairing operators. Detailed proposals for measuring collective modes and how they affect states inside the vortex core will be considered in a future work. We strongly believe that the identification of charge $4e^-$ pairing will provide compelling evidence of topological pairing mechanism and duality.

Acknowledgments

This work was supported by the National Science Foundation MRSEC program (DMR-1720139) at the Materials Research Center of Northwestern University. A part of this work was performed at the Aspen Center for Physics, which is supported by National Science Foundation grant PHY-1607611.

[1] R. Rajaraman, *Solitons and instantons* (North-Holland, Netherlands, 1982), ISBN 0-444-86229-3, URL `http://inis.iaea.org/search/search.aspx?orig_q=RN:15036991`.

[2] J. Goldstone and F. Wilczek, Phys. Rev. Lett. **47**, 986 (1981), URL `https://link.aps.org/doi/10.1103/PhysRevLett.47.986`.

[3] T. Jaroszewicz, Physics Letters B **146**, 337 (1984), ISSN 0370-2693, URL `https://www.sciencedirect.com/science/article/pii/0370269384917088`.

[4] T. Jaroszewicz, Physics Letters B **159**, 299 (1985), ISSN 0370-2693, URL `https://www.sciencedirect.com/science/article/pii/0370269385902540`.

[5] Y.-H. CHEN and F. WILCZEK, International

Journal of Modern Physics B **03**, 117 (1989), https://doi.org/10.1142/S0217979289000117, URL https://doi.org/10.1142/S0217979289000117.
[6] A. Abanov and P. Wiegmann, Nuclear Physics B **570**, 685 (2000), ISSN 0550-3213, URL https://www.sciencedirect.com/science/article/pii/S0550321399008202.
[7] A. Tanaka and X. Hu, Phys. Rev. Lett. **95**, 036402 (2005), URL https://link.aps.org/doi/10.1103/PhysRevLett.95.036402.
[8] T. Senthil and M. P. A. Fisher, Phys. Rev. B **74**, 064405 (2006), URL https://link.aps.org/doi/10.1103/PhysRevB.74.064405.
[9] T. Grover and T. Senthil, Phys. Rev. Lett. **100**, 156804 (2008), URL https://link.aps.org/doi/10.1103/PhysRevLett.100.156804.
[10] H. Yao and D.-H. Lee, Phys. Rev. B **82**, 245117 (2010), URL https://link.aps.org/doi/10.1103/PhysRevB.82.245117.
[11] L. Fu, S. Sachdev, and C. Xu, Phys. Rev. B **83**, 165123 (2011), URL https://link.aps.org/doi/10.1103/PhysRevB.83.165123.
[12] I. F. Herbut, C.-K. Lu, and B. Roy, Phys. Rev. B **86**, 075101 (2012), URL https://link.aps.org/doi/10.1103/PhysRevB.86.075101.
[13] C.-K. Lu and I. F. Herbut, Phys. Rev. Lett. **108**, 266402 (2012), URL https://link.aps.org/doi/10.1103/PhysRevLett.108.266402.
[14] E.-G. Moon, Phys. Rev. B **85**, 245123 (2012), URL https://link.aps.org/doi/10.1103/PhysRevB.85.245123.
[15] C.-H. Hsu and S. Chakravarty, Phys. Rev. B **87**, 085114 (2013), URL https://link.aps.org/doi/10.1103/PhysRevB.87.085114.
[16] P. Goswami and Q. Si, Phys. Rev. B **89**, 045124 (2014), URL https://link.aps.org/doi/10.1103/PhysRevB.89.045124.
[17] P. Goswami and Q. Si, Phys. Rev. B **95**, 224438 (2017), URL https://link.aps.org/doi/10.1103/PhysRevB.95.224438.
[18] C.-C. Liu, P. Goswami, and Q. Si, Phys. Rev. B **96**, 125101 (2017), URL https://link.aps.org/doi/10.1103/PhysRevB.96.125101.
[19] T. Senthil, A. Vishwanath, L. Balents, S. Sachdev, and M. P. A. Fisher, Science **303**, 1490 (2004), ISSN 0036-8075, https://science.sciencemag.org/content/303/5663/1490.full.pdf, URL https://science.sciencemag.org/content/303/5663/1490.
[20] A. Nahum, P. Serna, J. T. Chalker, M. Ortuño, and A. M. Somoza, Phys. Rev. Lett. **115**, 267203 (2015), URL https://link.aps.org/doi/10.1103/PhysRevLett.115.267203.
[21] C. Wang, A. Nahum, M. A. Metlitski, C. Xu, and T. Senthil, Phys. Rev. X **7**, 031051 (2017), URL https://link.aps.org/doi/10.1103/PhysRevX.7.031051.
[22] Z. Wang, M. P. Zaletel, R. S. K. Mong, and F. F. Assaad, Phys. Rev. Lett. **126**, 045701 (2021), URL https://link.aps.org/doi/10.1103/PhysRevLett.126.045701.
[23] Y. Cao, V. Fatemi, S. Fang, K. Watanabe, T. Taniguchi, E. Kaxiras, and P. Jarillo-Herrero, Nature **556**, 43 (2018), ISSN 1476-4687, URL https://doi.org/10.1038/nature26160.
[24] M. Yankowitz, S. Chen, H. Polshyn, Y. Zhang, K. Watanabe, T. Taniguchi, D. Graf, A. F. Young, and C. R. Dean, Science **363**, 1059 (2019), ISSN 0036-8075, https://science.sciencemag.org/content/363/6431/1059.full.pdf, URL https://science.sciencemag.org/content/363/6431/1059.
[25] X. Lu, P. Stepanov, W. Yang, M. Xie, M. A. Aamir, I. Das, C. Urgell, K. Watanabe, T. Taniguchi, G. Zhang, et al., Nature **574**, 653 (2019).
[26] P. Stepanov, I. Das, X. Lu, A. Fahimniya, K. Watanabe, T. Taniguchi, F. H. L. Koppens, J. Lischner, L. Levitov, and D. K. Efetov, Nature **583**, 375 (2020), ISSN 1476-4687, URL https://doi.org/10.1038/s41586-020-2459-6.
[27] Y. Saito, J. Ge, K. Watanabe, T. Taniguchi, and A. F. Young, Nature Physics **16**, 926 (2020), ISSN 1745-2481, URL https://doi.org/10.1038/s41567-020-0928-3.
[28] A. Kerelsky, L. J. McGilly, D. M. Kennes, L. Xian, M. Yankowitz, S. Chen, K. Watanabe, T. Taniguchi, J. Hone, C. Dean, et al., Nature **572**, 95 (2019), ISSN 1476-4687, URL https://doi.org/10.1038/s41586-019-1431-9.
[29] Y. Choi, J. Kemmer, Y. Peng, A. Thomson, H. Arora, R. Polski, Y. Zhang, H. Ren, J. Alicea, G. Refael, et al., Nature Physics **15**, 1174 (2019), ISSN 1745-2481, URL https://doi.org/10.1038/s41567-019-0606-5.
[30] Y. Jiang, X. Lai, K. Watanabe, T. Taniguchi, K. Haule, J. Mao, and E. Y. Andrei, Nature **573**, 91 (2019), ISSN 1476-4687, URL https://doi.org/10.1038/s41586-019-1460-4.
[31] Y. Xie, B. Lian, B. Jäck, X. Liu, C.-L. Chiu, K. Watanabe, T. Taniguchi, B. A. Bernevig, and A. Yazdani, Nature **572**, 101 (2019), ISSN 1476-4687, URL https://doi.org/10.1038/s41586-019-1422-x.
[32] D. Wong, K. P. Nuckolls, M. Oh, B. Lian, Y. Xie, S. Jeon, K. Watanabe, T. Taniguchi, B. A. Bernevig, and A. Yazdani, Nature **582**, 198 (2020), ISSN 1476-4687, URL https://doi.org/10.1038/s41586-020-2339-0.
[33] U. Zondiner, A. Rozen, D. Rodan-Legrain, Y. Cao, R. Queiroz, T. Taniguchi, K. Watanabe, Y. Oreg, F. von Oppen, A. Stern, et al., Nature **582**, 203 (2020), ISSN 1476-4687, URL https://doi.org/10.1038/s41586-020-2373-y.
[34] X. Liu, Z. Wang, K. Watanabe, T. Taniguchi, O. Vafek, and J. I. A. Li, Science **371**, 1261 (2021), ISSN 0036-8075, https://science.sciencemag.org/content/371/6535/1261.full.pdf, URL https://science.sciencemag.org/content/371/6535/1261.
[35] Y. Cao, D. Rodan-Legrain, J. M. Park, N. F. Q. Yuan, K. Watanabe, T. Taniguchi, R. M. Fernandes, L. Fu, and P. Jarillo-Herrero, Science **372**, 264 (2021), ISSN 0036-8075, https://science.sciencemag.org/content/372/6539/264.full.pdf, URL https://science.sciencemag.org/content/372/6539/264.
[36] F. Wu, A. H. MacDonald, and I. Martin, Phys. Rev. Lett. **121**, 257001 (2018), URL https://link.aps.org/doi/10.1103/PhysRevLett.121.257001.
[37] H. Isobe, N. F. Q. Yuan, and L. Fu, Phys. Rev. X **8**, 041041 (2018), URL https://link.aps.org/doi/10.1103/PhysRevX.8.041041.
[38] B. Lian, Z. Wang, and B. A. Bernevig, Phys. Rev. Lett. **122**, 257002 (2019), URL https://link.aps.org/doi/10.1103/PhysRevLett.122.257002.
[39] Y.-Z. You and A. Vishwanath, npj Quantum Materials **4**, 16 (2019), ISSN 2397-4648, URL https://doi.org/10.1038/s41535-019-0153-4.
[40] L. Classen, A. V. Chubukov, C. Honerkamp, and M. M. Scherer, Phys. Rev. B **102**, 125141 (2020), URL https:

//link.aps.org/doi/10.1103/PhysRevB.102.125141.

[41] D. V. Chichinadze, L. Classen, and A. V. Chubukov, Phys. Rev. B **102**, 125120 (2020), URL https://link.aps.org/doi/10.1103/PhysRevB.102.125120.

[42] V. Kozii, M. P. Zaletel, and N. Bultinck (2020), 2005.12961.

[43] Y. Wang, J. Kang, and R. M. Fernandes, Phys. Rev. B **103**, 024506 (2021), URL https://link.aps.org/doi/10.1103/PhysRevB.103.024506.

[44] E. Khalaf, S. Chatterjee, N. Bultinck, M. P. Zaletel, and A. Vishwanath, Science Advances **7**, eabf5299 (2021), ISSN 2375-2548, URL http://dx.doi.org/10.1126/sciadv.abf5299.

[45] M. Christos, S. Sachdev, and M. S. Scheurer, Proceedings of the National Academy of Sciences **117**, 29543 (2020).

[46] S. Chatterjee, M. Ippoliti, and M. P. Zaletel (2020), 2010.01144.

[47] E. Khalaf, P. Ledwith, and A. Vishwanath (2020), 2012.05915.

[48] F. D. M. Haldane, Phys. Rev. Lett. **61**, 1029 (1988), URL https://link.aps.org/doi/10.1103/PhysRevLett.61.1029.

[49] G. Murthy and S. Sachdev, Nuclear Physics B **344**, 557 (1990), ISSN 0550-3213, URL https://www.sciencedirect.com/science/article/pii/0550321390906709.

[50] N. Read and S. Sachdev, Phys. Rev. B **42**, 4568 (1990), URL https://link.aps.org/doi/10.1103/PhysRevB.42.4568.

[51] T. Schäfer and E. V. Shuryak, Rev. Mod. Phys. **70**, 323 (1998), URL https://link.aps.org/doi/10.1103/RevModPhys.70.323.

[52] D. Diakonov, Progress in Particle and Nuclear Physics **51**, 173 (2003), ISSN 0146-6410, URL https://www.sciencedirect.com/science/article/pii/S0146641003900147.

[53] G. 't Hooft, Phys. Rev. D **14**, 3432 (1976), URL https://link.aps.org/doi/10.1103/PhysRevD.14.3432.

[54] R. Bistritzer and A. MacDonald, Proceedings of the National Academy of Sciences **108**, 12233 (2011).

[55] R. D. Gail, M. Goerbig, F. Guinea, G. Montambaux, and A. Neto, Physical Review B **84**, 045436 (2011).

[56] J. M. B. Lopes dos Santos, N. M. R. Peres, and A. H. Castro Neto, Phys. Rev. B **86**, 155449 (2012), URL https://link.aps.org/doi/10.1103/PhysRevB.86.155449.

[57] H. C. Po, L. Zou, A. Vishwanath, and T. Senthil, Phys. Rev. X **8**, 031089 (2018), URL https://link.aps.org/doi/10.1103/PhysRevX.8.031089.

[58] A. H. Castro Neto, F. Guinea, N. M. R. Peres, K. S. Novoselov, and A. K. Geim, Rev. Mod. Phys. **81**, 109 (2009), URL https://link.aps.org/doi/10.1103/RevModPhys.81.109.

[59] A. Polyakov and A. Belavin, Jetp Letters **22**, 503 (1975).

[60] J. Arafune, P. G. O. Freund, and C. J. Goebel, Journal of Mathematical Physics **16**, 433 (1975), https://aip.scitation.org/doi/pdf/10.1063/1.522518, URL https://aip.scitation.org/doi/abs/10.1063/1.522518.

[61] R. Jackiw and C. Rebbi, Phys. Rev. D **13**, 3398 (1976), URL https://link.aps.org/doi/10.1103/PhysRevD.13.3398.

[62] C. J. Callias, Phys. Rev. D **16**, 3068 (1977), URL https://link.aps.org/doi/10.1103/PhysRevD.16.3068.

[63] C. Callias, Communications in Mathematical Physics **62**, 213 (1978), ISSN 1432-0916, URL https://doi.org/10.1007/BF01202525.

[64] J. Kang and O. Vafek, Phys. Rev. Lett. **122**, 246401 (2019), URL https://link.aps.org/doi/10.1103/PhysRevLett.122.246401.

[65] K. Seo, V. N. Kotov, and B. Uchoa, Phys. Rev. Lett. **122**, 246402 (2019), URL https://link.aps.org/doi/10.1103/PhysRevLett.122.246402.

[66] Y.-H. Zhang, H. C. Po, and T. Senthil, Phys. Rev. B **100**, 125104 (2019), URL https://link.aps.org/doi/10.1103/PhysRevB.100.125104.

[67] J. Kang and O. Vafek, Phys. Rev. B **102**, 035161 (2020), URL https://link.aps.org/doi/10.1103/PhysRevB.102.035161.

[68] Y. Da Liao, J. Kang, C. N. Breiø, X. Y. Xu, H.-Q. Wu, B. M. Andersen, R. M. Fernandes, and Z. Y. Meng, Phys. Rev. X **11**, 011014 (2021), URL https://link.aps.org/doi/10.1103/PhysRevX.11.011014.

[69] E. Demler, W. Hanke, and S.-C. Zhang, Rev. Mod. Phys. **76**, 909 (2004), URL https://link.aps.org/doi/10.1103/RevModPhys.76.909.